EUROPEAN ORGANIZATION FOR NUCLEAR RESEARCH

CERN/EP 82-165
3 November 1982

($q\bar{q}$) SPECTROSCOPY AND SEARCH FOR GLUEBALLS, BARYONIA AND OTHER BOSON RESONANCES IN $\bar{p}p$ ANNIHILATIONS AT REST WITH THE ASTERIX EXPERIMENT AT LEAR

The ASTERIX Collaboration(*)

S. Ahmad[4], C. Amsler[6], R. Armenteros[1], E. Auld[5], D. Axen[5], G. Beer[5], J.C. Bizot[4], M. Caria[6], M. Comyn[5], W. Dahme[3], B. Delcourt[4], K. Erdman[5], P. Eschtruth[4], U. Gastaldi[2], M. Heel[2], R. Howard[5], J. Jeanjean[4], H. Kalinowsky[2], F. Kayser[2], E. Klempt[2], R. Landua[2], H. Nguyen[4], L. Robertson[5], C. Sabev[1], R. Schneider[2], O. Schreiber[2], U. Straumann[6], P. Truöl[6], B. White[5] and W.R. Wodrich[3]

(Presented by W. Dahme)

INTRODUCTION

This enlarged version of the presentation made at the Workshop refers to the general search for boson resonances produced in $\bar{p}p$ annihilations at rest to be made as part of the ASTERIX experiment at LEAR.

Firstly, the results of different theoretical models proposing the existence of non ($q\bar{q}$) states (baryonium, glueballs, hybrids, four-quark resonances) will be summarized. A short description of some of the problems still remaining in the interpretation and classification of SU(3) nonets will follow. Then the main components of the apparatus together with their expected performances will be presented. Finally, the results of a Monte-Carlo simulation of the annihilation $p\bar{p} \to \gamma B(\pi^+\pi^-)$ will be given as an illustration of the mass resolution and detection sensitivity which can be attained with the apparatus.

Invited paper at the Workshop on Physics at
LEAR With Low Energy Cooled Antiprotons
9-16 May 1982, Erice, Sicily

(*) CERN[1], Mainz[2], Munich[3], Orsay[4] (LAL), Vancouver-Victoria-TRIUMF[5], Zurich[6]

0936P/RA/ed

THEORETICAL BACKGROUND

Although we attempt to summarize the results obtained from the main existing models on non ($q\bar{q}$) states, special emphasis will be put on those inspired by QCD principles. This not only because they constitute the largest theoretical work in the field but also because we have considered it useful to collect results which are still widely dispersed in the literature.

Potential models

Since the results of these models have been frequently reviewed [1], an extensive summary is not required. The following remarks are abstracted from the nice and comprehensive presentation by Dover and Richard at the Barr Symposium [2]. No doubt, other speakers will bring it up to date at this Workshop.

The starting point of the models is to notice that the long and medium ranges of the $N\bar{N}$ potential are due to the exchange of the same bosons responsible for the NN forces. Various phenomenological NN potentials are considered and transposed to the $N\bar{N}$ case reversing the sign of the exchange contributions with odd G-parity while keeping the same sign for those with even G-parity. The $N\bar{N}$ potential is then found to be more attractive than the NN one and many states are obtained close and below the $N\bar{N}$ threshold. How these results are affected by the $N\bar{N}$ annihilation contribution is not clear; depending on the parametrisation it can destroy the spectrum built up from the real part of the potential or leave unaffected some parts of it.

Dover and Richard point out that, taking into proper consideration the spin dependence of the real potential, the effect of a change in the annihilation short range potential is to move the whole spectrum up or down with little change in the ordering of the different levels. A brief summary of the results obtained is:

(a) There are channels where the different exchange forces are coherently attractive. The most spectacular being in the I = 0 natural parity sector i.e. the states $^{1}{}^{3}P_{0}$, $^{1}{}^{3}S_{1} + {}^{1}{}^{3}D_{1}$, $^{1}{}^{3}P_{2} + {}^{1}{}^{3}F_{2}$ appear as bound states.

(b) On the contrary, there are channels where the spin-dependent parts of the potential are repulsive and compete with the attraction mainly due to ω exchange. Bound states are considered unlikely to be seen in these channels e.g. in the I = 0, spin triplet sequence $^{1}{}^{3}P_{1}$, $^{1}{}^{3}D_{2}$, etc.

(c) There are channels in which the existence of bound states depends critically on the details of the model used. They would, in any case, have small binding energies and low orbital angular momentum. All I = 1 partial waves would appear to fall in this category; they would cluster near the $N\bar{N}$ threshold.

Binding energies depend strongly on the radius r_0 assumed for the short range potential. For $r_0 \sim 0.8$ fm the three lowest states (0^{++}, 1^{--} and 2^{++}) appear in the region where Fransson et al. [3] have observed monochromatic γ-rays: in the 160-450 MeV binding energy region. For $r_0 = 0.6$ fm some of the I = 1 P states lie between 200-400 MeV while the 0^{++}, 1^{--} and 2^{++} states are very deeply bound and probably very wide.

Clearly these models do not have yet a precise predictive power. Experiments at LEAR studying the production of monochromatic γ's and π's, X-ray transitions and the low energy properties of the different cross sections should provide much needed input data to improve the parameters governing the models.

QCD inspired models

As is well known, QCD explains the forces between quarks through the exchange of gluons: massless, coloured vector particles which interact not only with the quarks but also with each other. It is this remarkable last property that leads to the belief that quarkless hadrons should exist composed of bound states of gluons. They go by the name of glueballs or gluonium. Their more general properties follow from QCD principles. Namely, to be observable they should be colour singlets, like quark states; since gluons have no isospin or electric charge, glueballs should have I = 0 and Q = 0. The gluon-quark coupling being independent of the quark flavour, glueballs should be singlets of SU(3) flavour. A two gluon state has charge conjugation C = +1, a three gluon state can have C = +1 or C = -1 depending on whether their colour coupling is anti-symmetric or symmetric.

Finally, because glueballs are bosons their wave functions have to be totally symmetric under the interchange of space, spin and colour degrees of freedom.

More specific properties like spin-parity (J^{PC}), masses and partial decay widths depend on the dynamics of gluons to form hadrons. Although T. Barnes [4] has already reviewed and commented on some of the existing models, it may be useful to enumerate in some detail their main results. The large amount of theoretical work devoted to glueballs together with the diversity of the results often obtained, enhances the interest and importance of an intensive experimental search for them.

J^{PC} proposals for two and three gluon states

The simplest models [5] consider two non-interacting gluons moving in a potential with an orbital angular momentum L; the resulting spin, parity and charge conjugation, J^{PC}, being:

$$L = 0: \quad 0^{++}, \ 2^{++}; \quad L = 1: \quad 0^{-+}, \ 1^{-+}, \ 2^{-+}; \quad L = 2: \quad 2^{++}, \ 0^{++}$$

The appearance of a $J^{PC} = 1^{-+}$ state has to be noted since it cannot be obtained from a $(q\bar{q})$ combination. However, two massless and therefore transverse gluons, like 2 photons, cannot couple to give a spin 1 state. It is nevertheless argued that confinement gives gluons an effective mass allowing them to be also longitudinally polarised [5]. Virtual gluons, it is counter-argued [6(a,b)], remain transverse because of general principles of gauge and Lorentz invariance.

With the exception of the 1^{-+} state, the MIT bag model arrives at the same set of states [6(a)]. It considers free gluon fields confined in a static spherical cavity and obtains as gluon eigenmodes both transverse electric (TE) solutions with parity $-(-1)^{\ell}$ and transverse magnetic (TM) solutions with parity $(-1)^{\ell}$. No solutions with $\ell = 0$ are obtained and the lowest energy state found is the $\ell = 1$ TE mode (1^{+}) followed, in increased order of energy, by the $\ell = 2$ TE mode (2^{-}) and the $\ell = 1$ TM mode (1^{-}). The resulting J^{PC} for the gluonium ground state is obtained from the $1^{+} \times 1^{+}$ combination: 0^{++}, 2^{++}. For the first excited states the 1^{+} lower energy configuration is combined alternatively with the 2^{-} and 1^{-} modes to obtain the series: 3^{-+}, 2^{-+}, 1^{-+}, 2^{-+}, 1^{-+}, 0^{-+}. With the exception of the 2^{-+} and 0^{-+} these states are, however, spurious and arise from translations of the 2g centre of mass system within the confining bag. Similarly extraneous states occur when one considers 3g states either in the bag model or in potential models. Those J^{PC} left are given in table 1 for the two models. States not accessible to $q\bar{q}$ are indicated by a box:

Table 1. J^{PC} proposals for three gluon states

	Bag model	Potential model
Ground states	0^{++}; 1^{+-}; 3^{--}	0^{-+}; 1^{--}; 3^{--}
Excited states	$\boxed{1^{-+}}$; 2^{-+}; 3^{-+}	$\boxed{0^{+-}}$; 1^{+-}; $\boxed{2^{+-}}$; 3^{+-}
	0^{-+}; 2^{--}; 2^{--}	0^{++}; 1^{++}; 2^{++}; 3^{++}

The parity difference between the bag and potential models is due to the fact that in potential models the lowest gluon mode is an 1^-, $\ell = 0$ state while in the bag model it is an 1^+, $\ell = 1$ state. Although this difference has its origin - like in the two gluon case - on whether the gluons have to be considered effectively as massless or not, deeper invariance principles appear to be involved about the validity of considering longitudinal gluons.

Masses

Few attempts have been made to calculate masses in potential models. Barnes [6(b)] has considered a model of two bound transverse gluons - therefore it does not allow a $J^{PC} = 1^{-+}$ state - and after introducing hyperfine effects finds degenerate 0^{-+} and 0^{++} ground states and a first 2^{++} excited state with a mass about 20% higher. The ground state mass, however, is not calculable because of the lack of knowledge about the long range colour octet-octet force.

In the bag model [6(a)], a naive calculation neglecting the spin-spin interactions finds two gluon states:

- ground state: $M(0^{++})$; $M(2^{++}) = 960$ MeV,
- first excited state: $M(0^{-+}; 2^{-+}) = 1300$ MeV,

and for 3 gluon states:

- ground state: $M(0^{++}; 1^{+-}; 3^{+-}) = 1450$ MeV,
- first excited state: $M(3^{-+}; 2^{-+}; \ldots) = 1800$ MeV.

Attempts to include spin effects in the 2g ground state appear to shift the 2^{++} mass up to 1300 MeV while that of the 0^{++} drops down unpleasantly to 100 MeV. The suggestion is made that this scalar glueball may mix with the vacuum to which the physical scalar glueball would be orthogonal. The expectation is then that the 0^{++} mass would be of the order of 1000 MeV.

Widths

A simple argument, first given by Robson [7], suggests that typical glueball hadronic widths, Γ_G, may be approximated by the geometrical mean of those for allowed and Zweig forbidden decays:

$$\Gamma_G = (\Gamma_a \Gamma_f)^{1/2}$$

It is assumed that Zweig forbidden decays require the annihilation of the initial $(q\bar{q})$ into a purely gluon intermediate state which subsequently materialises into a $(q\bar{q})$ pair; for a glueball only the last stage would be required. Γ_a and Γ_f being, respectively, of the order of 100 and 1 MeV, Γ_G is then expected to be of the order of 10 MeV.

Donoghue [8], on the other hand, has estimated that in the limit of large N_c for the $SU(N_c)$ colour group, glueball widths are suppressed by N_c^{-1} over those of quark states while they are enhanced by a factor N_F, where N_F is the number of light flavours. Using a model that incorporates this approach, Donoghue finds $\Gamma_G/\Gamma_{q\bar{q}} \sim 1/3$ for glueball masses $m \lesssim 2$ GeV.

Decay modes

If, as it is assumed, glueballs are SU(3) flavour singlets then they should couple equally to final states of all flavours satisfying the required conservation laws. This symmetry in glueball decay modes has been suggested as one of the possible tests to distinguish glueballs from $(q\bar{q})$ states.

A table of possible decay modes for glueballs of given J^{PC} has been given by Bjorken [9] and is reproduced in table 2.

Table 2. Decay modes accessible to glueballs of given J^{PC} [9]

Type	J^{PC}	Typical decays
(1) E_iE_j	0^{++}; 2^{++}	$\pi\pi$; $K\bar{K}$; $\eta\eta$; $\eta'\eta'$; $\rho\rho$; $\omega\omega$; $K^*\bar{K}^*$; $\phi\phi$
(2) E_iB_j	0^{-+}; 1^{-+}; 2^{-+}	$\pi\delta$, $\bar{K}\kappa$; ηS^*; $\eta'\epsilon$; ρB; TA_1; K^*Q; ...
(3) B_iB_j	0^{++}; 2^{++}	Same as (1)
(4) $E_iE_jB_k$	0^{-+}; 1^{--}; 3^{--}	$\pi\delta$; $\bar{K}\kappa$; $\eta'\epsilon$; $\pi\rho$; $K\bar{K}^*$; $\eta\omega$; $\eta'\phi$; ωf; ...
(5) $E_iE_jB_k$	0^{++}; 1^{++}; 2^{++}	Same as (1) + $\pi\delta$; $\bar{K}\kappa$; ηS^*; ...
	1^{+-}; 2^{+-}; 3^{+-}	$\pi\rho$; $\bar{K}K^*$; $\eta\omega$; $\eta'\phi$; πB; $\bar{K}Q$; ηD; ...
(6) $E_iB_jB_k$	0^{-+}; 1^{-+}; 2^{-+}	Same as (2)
	1^{--}; 2^{--}; 3^{--}	πB; $\bar{K}Q$; ρA_2; $\bar{K}^*K^{**}$; ωf; df'; ...
(7) $B_iB_jB_k$	0^{++}; 1^{+-}; 3^{+-}	Same as (1) + πB; $\bar{K}Q$; ρA_1; ρA_2; ...

E_i and B_i correspond to the TE and TM modes of the bag model.

Lipkin [10] has considered a number of SU(3) selection rules that could help to distinguish between glueballs and $(q\bar{q})$ states. From his very detailed considerations we summarize the following. Concerning quasi-two-body decays into strange particles, Lipkin notes that the unitary singlet components of $K\bar{K}$, $\bar{K}^*_V K^*_V$ and $K^*_T\bar{K}$ have charge conjugation C = +1, while those of $K^*_V\bar{K}$ and $K^*_V K^*_T$ have C = -1 (the indices V or T indicate the vector or tensor nature of the particle). The unitary octet components have, on the contrary, no definite C-value since both odd and even C states can be constructed using symmetric and antisymmetric, D and F, couplings.

Denoting by $g^{\pm}$ the C-value of the glueball and by $(q\bar{q})$ quarkonium, we have as allowed decays:

$$g^+ \rightarrow K\bar{K},\ K^*_V\bar{K}^*_V \quad \text{and} \quad K^*_T\bar{K}$$

$$g^- \rightarrow K^*_V\bar{K} \quad \text{and} \quad K\bar{K}^*_T$$

$$(q\bar{q}) \rightarrow \text{all the above}$$

Thus, while an even C quarkonium like the f' can decay into $K\bar{K}$ and $K^*_V\bar{K}$, a glueball with the same quantum numbers would decay only into $K\bar{K}$ but not into $K^*_V\bar{K}$.

Lipkin then considers decays involving π, ρ, ω and ϕ and points out that because of the Zweig rule ideally mixed quarkonium cannot go into $\omega\omega$, $\omega\eta$, $\rho\rho$, $\rho\pi$ or $\pi\pi$ if composed of $(s\bar{s})$ or into $\phi\phi$ or $\phi\eta$ if composed of $(u\bar{u}, d\bar{d})$ quarks. Depending on the C conjugation, glueballs can decay as follows:

$$g^+ \rightarrow \omega\omega,\ \phi\phi,\ \rho\rho,\ \pi\pi$$

$$g^- \rightarrow \omega\eta,\ \phi\eta,\ \rho\pi,$$

The combination of these decays together with those given before for $K\bar{K}$ and $(K^*\bar{K})$ pairs can, in principle, provide a good distinction between $(q\bar{q})$ and glueball states if the masses are above the relevant thresholds.

A number of authors, e.g. [11] and references therein, have pointed out that there are particles or states that appear to have a particularly strong coupling to gluons. Looking for final states containing them may therefore enhance the probability of finding glueballs. The η, η', $(\pi\pi)$ in an S-wave, f(1270) and $(\phi\phi)$ are the

most often quoted "high glue" states. Fairly complex arguments - for an experimentalist - lead to this conclusion, they are substantiated by the observation that the branching ratios $\psi \to \eta\gamma$, $\eta'\gamma$ and $\psi \to f\gamma$, $\psi' \to \psi(\pi\pi)_S$ are observed to be unexpectedly high unless large glue matrix elements are invoked for these states.

Following these observations the final states given in table 3 together with their J^{PC} might facilitate the search for glueballs.

Table 3. J^{PC} available for favoured glueball decays [11]

$\eta\eta$	$\to 0^{++}, 2^{++}$
$\eta'\eta'$	
$\eta\eta'$	$\to 0^{++}, 1^{-+}, 2^{++}$
$\eta(\pi\pi)_S$	$\to 0^{-+}, 1^{++}, 2^{-+}$
$(\pi\pi)_S(\pi\pi)_S$	$\to 0^{++}, 1^{-+}, 2^{++}$
ηf	$\to 2^{-+}$

Lattice theories

Much theoretical work is being devoted to Monte-Carlo calculations within the frame of lattice gauge theories to predict the QCD glueball spectrum. Because this is considered to be a most promising field although still in a fluid but fast advancing state, a separate section is devoted to it using the latest results [12] we are aware of. They appear to illustrate well the generality of the results obtained by the different groups, who, it has to be underlined, all insist on the large uncertainties involved in the calculations.

The ground state is found to be a $J^{PC} = 0^{++}$ state with a mass which cannot be calculated because of as yet insufficient knowledge about intervening parameters. However, estimates of the masses of excited states relative to that of the 0^{++} appear to be possible with relatively small uncertainty. They are given below in units of the $M(0^{++})$ mass:

$M(0^{++}) = 1$

$M(2^{++}) = 2.93 \pm 0.07$

$M(3^{++}) = 3.14 \pm 0.13$

$M(2^{-+}) = 3.47 \pm 0.17$

$M(3^{+-}) = 3.7 \pm 0.3$

$M(0^{--}) = 4.6 \begin{smallmatrix} +1.7 \\ -0.6 \end{smallmatrix}$

$M(2^{--}) = 4.8 \begin{smallmatrix} +1.0 \\ -0.5 \end{smallmatrix}$

Associating the lattice mass scale to the string tension, a $M(0^{++}) = (920 \pm 310)$MeV is obtained and the conjecture made that it could correspond to the $\varepsilon(700)$; the I = 0 scalar $(\pi\pi)$ found sometimes in partial wave analyses.

Before closing this section on glueball models mention has to be done of that of the ITEP group because it gives results vastly different to most existing ones. Using their QCD sum rule technique, Novikov and coworkers [13] find a mass $\sim$ 1300 MeV for the $J^{PC} = 2^{++}$ glueball while the scalar and pseudoscalar masses are estimated to be 2000 to 2500 MeV. Pascual and Tarrach [14] estimate that the sum rules would lead to widths of $\sim$ 700 MeV, making hopeless their experimental detection.

Hybrid $q\bar{q}g$ mesons

Although the expected characteristics of these states have been thoroughly discussed at this workshop by T. Barnes [4], it may be worthwhile underlining that amongst the proposed states there is an exotic one with $J^{PC} = 1^{-+}$ at a mass of about 1300 MeV. Barnes, encouragingly, suggests that it could be produced in

$$\bar{p}p \to H(I = 1)\pi$$

and decay into

$$H \to \eta\pi$$

Another possibility [15] is the existence of an I = 0 $J^{PC} = 1^{-+}$ state that decays, via an I = 1 $J^{PC} = 0^{-+}$ hybrid into four pions

$$1^{-+}(I = 0) \to \pi + 0^{-+}(I = 1) \to 4\pi.$$

This interesting possibility arises because the mass difference between the two hybrids is predicted to be of the order of the pion mass.

From bag model calculations including hyperfine effects, the following tentative mass assignments result

$0^{-+}(u\bar{u}g) \sim 1050$ MeV; $(u\bar{s}g) \sim 1200$ MeV; $(s\bar{s}g) \sim 1350$ MeV

$1^{-+}(u\bar{u}g) \sim 1300$ MeV; $(u\bar{s}g) \sim 1450$ MeV; $(s\bar{s}g) \sim 1600$ MeV

with estimated uncertainties of $\sim \pm 150$ MeV.

$(qq\bar{q}\bar{q})$ states

In the MIT bag model multiquark states are described by the same dynamics as $(q\bar{q})$ mesons and (qqq) baryons. An extension of the methods that led to a fairly successful interpretation of the above mesons and baryons results in the two different types of $(qq\bar{q}\bar{q})$ states described below.

S wave $(q^2\bar{q}^2)$ states with orbital angular momentum L = 0 [16]

Using a spherical cavity containing S wave quarks and anti-quarks, many SU(3) flavour multiplets are obtained with spin-parity 0^+, 1^+ and 2^+. Besides $1 \oplus 8$ nonets, called crypto-exotics because their quantum numbers are identical to those obtained in the $(q\bar{q})$ system, the 10, $\overline{10}$ and 27 representations are obtained: they include therefore states with quantum numbers not accessible to $(q\bar{q})$; they are called exotics. Colour and spin dependent forces have the effect of giving masses to the exotic states far beyond the thresholds for decay into $(q\bar{q})$ pairs; these states then decay via a super-allowed Zweig transition - no intermediate $(q\bar{q})$ needs to be created - and should be very broad and therefore difficult to observe. The same forces tend, on the contrary, to lower the mass of the crypto-exotic states which should then be narrower, particularly if they contain an $s\bar{s}$ pair and their masses occur close to the $K\bar{K}$ threshold.

The ground state found turns out to be a $J^{PC} = 0^{++}$ scalar nonet with the following masses and quark contents:

$$\varepsilon(700) = u\bar{u}d\bar{d};\ S^*(993) = \frac{1}{\sqrt{2}}\, s\bar{s}(u\bar{u} + d\bar{d});\ \delta(976) = u\bar{d}s\bar{s};$$

$$\kappa(900) = u\bar{s}d\bar{d},\ \ldots$$

The states have been indicated with the symbols used in their usual assignment to the $(q\bar{q})$ scalar nonet. As it will be seen in a later section, the $(q\bar{q})$ assignment meets with serious problems.

Essentially the close mass degeneracy between the isovector δ and the isoscalar S^* suggests an ideal nonet with $S^* = 1/\sqrt{2}\ (u\bar{u} + d\bar{d})$ and $\varepsilon = s\bar{s}$. Experimentally, however, both δ and S^* couple strongly to $K\bar{K}$ while the ε couples much more strongly to $\pi\pi$ than to $K\bar{K}$.

Jaffe's suggestion is that the $(q^2\bar{q}^2)$ assignment for those mesons is a more natural one; the $\varepsilon \to \pi\pi$ and the $\kappa \to K\pi$ decays being super-allowed explains their broad width, while the narrow widths of the δ and S^* would be due to their mass being close to the threshold of their main $K\bar{K}$ decay mode. The $(q\bar{q})$ scalar nonet then is predicted to exist at masses close to that of the $(q\bar{q})$ tensor nonet.

The $(q\bar{q}q\bar{q})$ states with orbital angular momentum $L \neq 0$ [17]

Here an elongated bag with an s-wave diquark (qq) and an s-wave antidiquark $(\bar{q}\bar{q})$, situated at each extreme, are separated by an angular momentum barrier. If high enough this barrier suppresses the decay into normal $(q\bar{q})$ mesons. The colour properties of the diquark and antidiquark determine the decay properties. A diquark (antidiquark) has to be in the 6 or $\bar{3}$ ($\bar{6}$ or 3) colour representation. A colour singlet can only be produced by linking a 6 with an $\bar{6}$ or a 3 with a $\bar{3}$. The decay of these colour singlets is assumed to occur via some quark-pair creation mechanism, when the necessity to form colour singlets baryons leads to two different types of baryons. Thus, for the $3\text{-}\bar{3}$ baryonium, a quark from the created $q\bar{q}$ pair combines with the $\bar{3}$ diquark to form a colour singlet baryon; similarly the $\bar{q}$ can form an antibaryon with the antidiquark. This so-called true baryonium should decay into a baryon-antibaryon system and occur with normal hadronic width i.e. $\sim$ 100 MeV. Using the same colour arguments, the $6\text{-}\bar{6}$ baryonia can easily be seen not to couple to a $B\bar{B}$ pair - hence their name of mock baryonia. They are expected to be of narrow widths decaying mainly into other mock baryonia states and an additional pion.

As is well known, the statistically weak evidence obtained once for the observation of narrow $(p\bar{p})$ states has been withdrawn now as a result of new experiments both by the original and other experimenters. Another possible candidate, the S-meson observed in $p\bar{p}$ formation experiments, finds itself in a very unstable situation. Nevertheless, the persistance with which monochromatic γ rays are observed in $p\bar{p}$ annihilations and the strong evidence for resonant-like effects in the analysis of the differential cross sections $\bar{p}p \to \pi\pi$ with and without a polarized target offer a hope that extensive experiments over a wide energy range at LEAR will give a fairly definitive answer to the existence or non-existence of baryonia with masses below $\sim$ 2 GeV.

Situation of $(q\bar{q})$ states

Although the non-relativistic quark model has met with considerable - although puzzling - success in interpreting the general characteristics of $(q\bar{q})$ resonances neither the theoretical nor the experimental situation is clear everywhere.

The reasons for Jaffes' 1977 suggestion that the observed scalar mesons were not $(q\bar{q})$ states but $(qq\bar{q}\bar{q})$ have already been mentioned. Although the status of the I = 1 $\delta(976)$ and of the I =0 $S^*(993)$ has changed but little, the I = 1/2 $\kappa(900)$ is now preferred to have a mass of 1500 MeV and a width $\sim$ 250 MeV, while to the I = 0 $\varepsilon(700)$ a new I = 0 at M = 1425 and width $\sim$ 160 MeV is added or preferred, depending on the analysis. A new I = 1 state with a mass $\sim$ 1300 MeV and a width $\sim$ 300 MeV coupling to $K\bar{K}$ appears difficult to avoid in some of the analyses. Clearly, if all those scalar candidates are true they make more than one nonet. With the exception of the $\delta(976)$ and $S^*(993)$ all states are obtained from partial wave analyses requiring a fair number of approximations and resulting often in ambiguous solutions; for their resolution assumptions are made which, although reasonable, may not all be correct.

How to remedy this state of affairs is difficult to say, but it may be worthwhile to point out that interesting experimental results on $(\pi\pi)$ effects have been observed in $p\bar{p}$ annihilations studied with bubble chambers [18] and therefore with limited statistics. Their deeper study with much larger statistics is likely to be rewarding since knowledge of the initial state would greatly restrict the number and quantum numbers of contributing partial waves.

The status of other recognized nonets will now be reviewed briefly.

1^{++} nonet

The I = 1 A_1, I = 1/2 Q_A and I = 0 D and E-mesons are the normally proposed members of this nonet. After a long period of uncertainty, the A_1 appears to be firmly established but contradictory results are obtained for its mass: M = 1280 ± 30 MeV in diffractive processes [19] and M = 1041 ± 13 MeV in baryon exchange processes [20]. The Q_A is well established, although a good determination of its mixing properties with the 1^{+-} Q_B still requires a better determination of the decays of the observable Q_1 and Q_2.

The E-meson, however, is a stumbling block; it is clearly observed decaying almost exclusively into $K^*\bar{K}$ + c.c. in π^- reactions [21] but not in K^-p reactions. Thus, unless there is an unexpected large violation of the Zweig rule, it cannot be the $s\bar{s}$ member of the nonet; a possibility which would appear to be ruled out also by the unsatisfactory SU(3) fit obtained if included as the isoscalar companion to the D-meson.

2^{++} nonet

Although from the point of view of SU(3) this nonet is in good good shape, the f^0 width, $\Gamma = (178 \pm 7.4)$ MeV, would appear to be too large and the suggestion has been made that a 2^{++} glueball may be hiding under it [22].

1^{+-} nonet

The $B \to \omega\pi$ and the Q_B appear well established. While evidence [23] has been obtained recently in just one experiment for an $I = 0$ member decaying into $\pi^+\pi^-\pi^0$ with a mass (1190 ± 60)MeV and a width (320 ± 50)MeV, the missing $I = 0$ companion, mainly $s\bar{s}$ member, has not been reported anywhere. It would be expected to occur at a mass of $\sim$ 1450 MeV and to decay mainly into $\bar{K}^*K$ + c.c.

Conclusions

After having reviewed the proposals about the existence of non $(q\bar{q})$ states and indicated some of the problems still affecting $(q\bar{q})$ states, it should be clear that much interesting and non-trivial experimental work remains to be done in the field of light quark spectroscopy in a region of mass accessible to $\bar{p}p$ annihilations at rest. There is furthermore the intuitive feeling that these annihilations, involving both valence quarks and antiquarks and a large gluon content, should be a good production source for many of the proposed states. This intuition is perhaps backed by the fact that in the relatively small experimental work done with $p\bar{p}$ at rest (only 150 x 10^3 pion annihilations and about 40 x 10^3 $KK_n\pi$ annihilations have been analyzed in bubble chamber experiments) much pioneer work on resonances was done. We think in particular of the $J^{PC} = 0^{-+}$ $(K\bar{K}\pi)$ and of the 1^{++} Q_1 $(K\pi\pi)$ states unravelled there already in the early sixties.

The outlook for experiments at LEAR appears bright although fraught with difficulties, amongst other things, due to the possibility that states with the same spin and parity, say glueballs and $(q\bar{q})$ states, may mix and add further complication to the general problem of attributing the correct components to the observed states.

THE APPARATUS AND ITS EXPECTED PERFORMANCE

The main features and expected performances of the different components of the apparatus will be briefly described. For fuller details we refer to our CERN Proposal [24]. A side and a front view of the experimental set-up are shown in fig. 1.

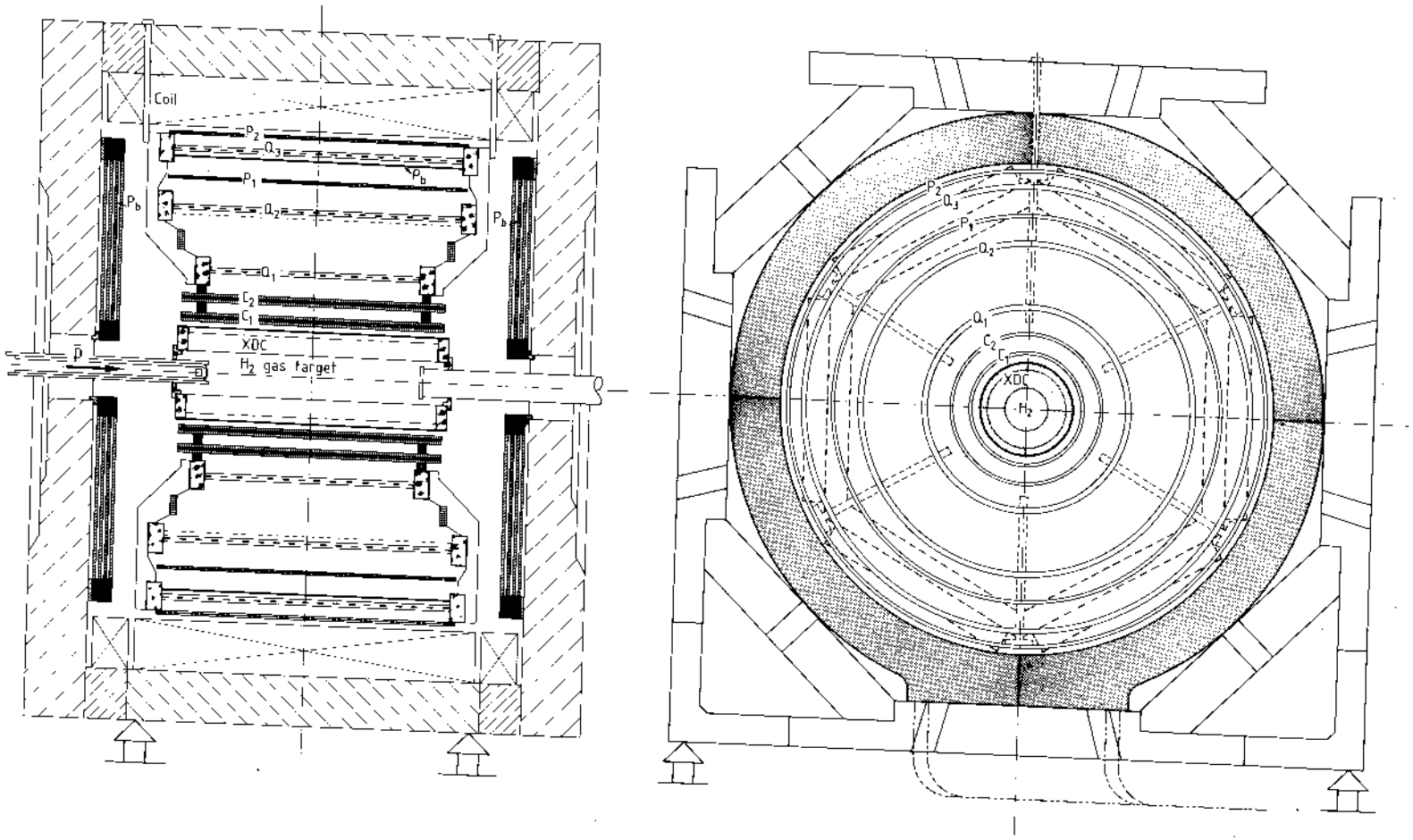

Fig. 1. Side and front view of the ASTERIX detector

Identification of the initial protonium state

Although this part of the set-up has been described in detail by U. Gastaldi [25], it is worthwhile recalling here that it consists of an X-ray drift chamber surrounding the hydrogen gas target from which it is separated by a thin (6 μ) mylar membrane. It is of cylindrical shape with dimensions: 30 cm diameter, 90 cm length and has a solid angle coverage of 0.9 x 4 π. It has an energy resolution of ± 10% at 10 keV and an overall detection efficiency of more than 50% in the X-ray energy range from 1.4 keV to 12 keV. Transitions to the S, P and D levels of the $\bar{p}p$ system should therefore be detectable and thus the quantum numbers of the annihilation state will be very much constrained.

Charged particle detection and momentum determination

A magnetic field will be provided by the solenoid of the DM1 magnetic detector [26] built at LAL (Orsay) and already successfully operated there. For its use at LEAR it has been slightly lengthened; it can provide a magnetic field up to 0.8 T which is uniform to better than ± 1% over a cylindrical volume of 177 cm diameter and 100 cm length.

Charged particle detection will be made with seven cylindrical multiwire proportional chambers; three (Q_1, Q_2 and Q_3 in the fig. 1) have already been used in the DM1 detector.

A cut away view showing the principal components of one of the Q chambers is shown in fig. 2. The main characteristics of each chamber are given in table 4.

Table 4. Characteristics of the cylindrical proportional chambers

		C_1	C_2	Q_1	Q_2	P_1	Q_3	P_2
Useful length	(mm)	800	800	756	1040	1020	1040	1040
Anode diameter	(mm)	385	540	733.8	1188.8	1400	1610.8	1735
Gap	(mm)	6	6	6	6	6	6	6
Anode wire spacing	(mm)	2.1	2.21	2.001	1.945	2.29	2.196	2.03
Cathode wire spacing (Cylindrically) projected	(mm)	3.45	3.13	2.9	2.8		3.3	
Anode wire number		576	768	1152	1920	1920	2304	2688
Cathode wire number		2 x 288	2 x 384	2 x 576	2 x 960	0	2 x 1652	0
Cylindrically projected angle		35°	45°	46°44'	45°55'	0	49°23'	0

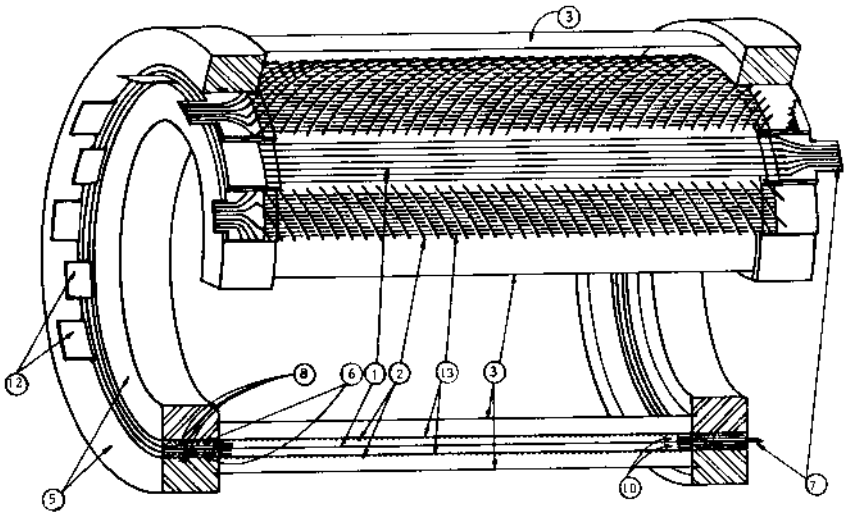

1) anode wires
2) cathode wires
3) mylar windows
5) aluminium frame
6) spacers
7) read-out connectors
8) O-ring gaskets
9) anode guard strips
10) fiber glass support strings for cathode wires

Fig. 2. Cut away view showing the principal components of the cylindrical MWPC's.

Five of the chambers will measure the r, ϕ and z coordinates of the particle crossing points while two (P_1 and P_2), lacking cathode read out, will measure r and ϕ only. Additional points will be obtained from the x-ray drift chamber.

The chamber characteristics and previous DM1 experience indicate that the charged particle crossing point should be determined with an accuracy given by: $\sigma(r.\phi) = \pm$ 0.6 mm and $\sigma(z) = \pm$ 1.5 mm. This should lead to a precision of $\pm$ 2 mm in the determination of the x, y and z coordinates of the $\bar{p}$ annihilation vertex.

The solid angle for best momentum measurements is $0.5 * 4\pi$, determined by the outermost chamber P_2. However, charged prong multiplicities can be obtained over 90% of the total 4π solid angle.

In the DM1 experiments the precision in the momentum determination was $\Delta p/p = \pm(2.5\ p/500)\%$ (p in MeV/c).

Insertion of a thin lead foil before Q_3 to increase γ detection worsens slightly the resolution to $\pm(3.5\ p/500)\%$ as shown in fig. 3 which is the result of a Monte-Carlo simulation.

Fig. 3. Momentum resolution for $\pi^{\pm}$ at 480 MeV/c (Monte-Carlo)

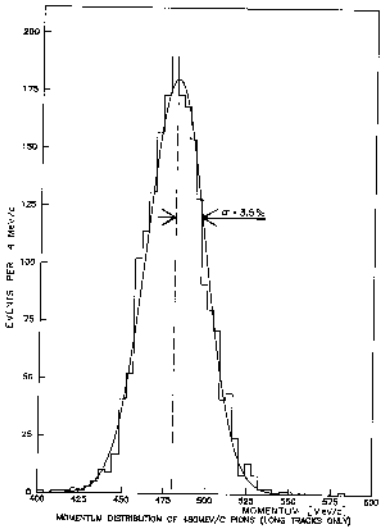

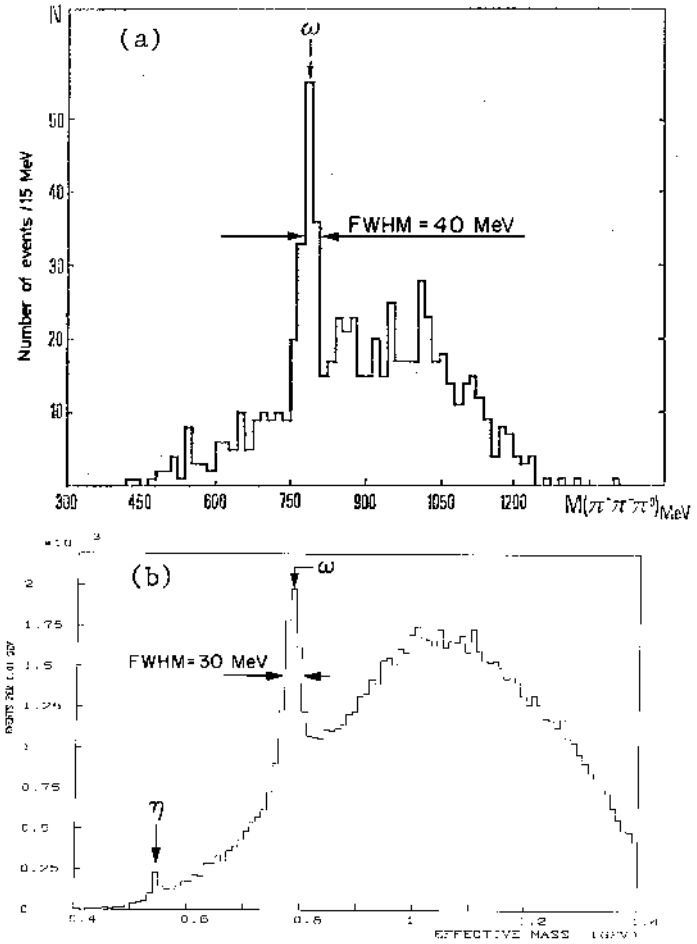

Fig. 4. Comparison of mass resolutions obtained for the ω meson in the DM1 spectrometer at Orsay (a) and in the Saclay Bubble Chamber at CERN (b).

An estimate of the resulting mass resolution may be obtained from inspection of the $(\pi^+\pi^-\pi^0)$ effective mass distribution obtained at Orsay in the reaction $e^+e^- \to 2\pi^+2\pi^-\pi^0$ at a total energy of 1650 MeV. In fig. 4(a) a clear ω signal is seen with a FWHM = 30 MeV; it agrees with the bubble chamber result in the annihilation at rest $\bar{p}p \to 2\pi^+2\pi^-\pi^0$ (fig. 4(b)). It has to be noted that in the DM1 data no adjustment of the measured quantities was made using kinematical fitting to the given final state. This was done for the bubble chamber data. The improved resolution achievable by the kinematic fitting will be illustrated below.

Gamma detection

The directions of emitted γ's will be determined by measuring their conversion points in a 0.9 radiation length lead converter, inserted between P_1 and Q_3. The forward and backward regions are covered by two endcap detectors.

Each endcap detector (fig. 5) consists of three hexagonal multiwire proportional chambers with a 0.9 radiation length lead converter between the first two chambers. The chamber in front of the converter serves to veto charged particles, while the γ shower from the converter is detected by coincidences between the second and third chambers using anode wire and cathode strip read out. The three chambers have the identical characteristics given in table 5.

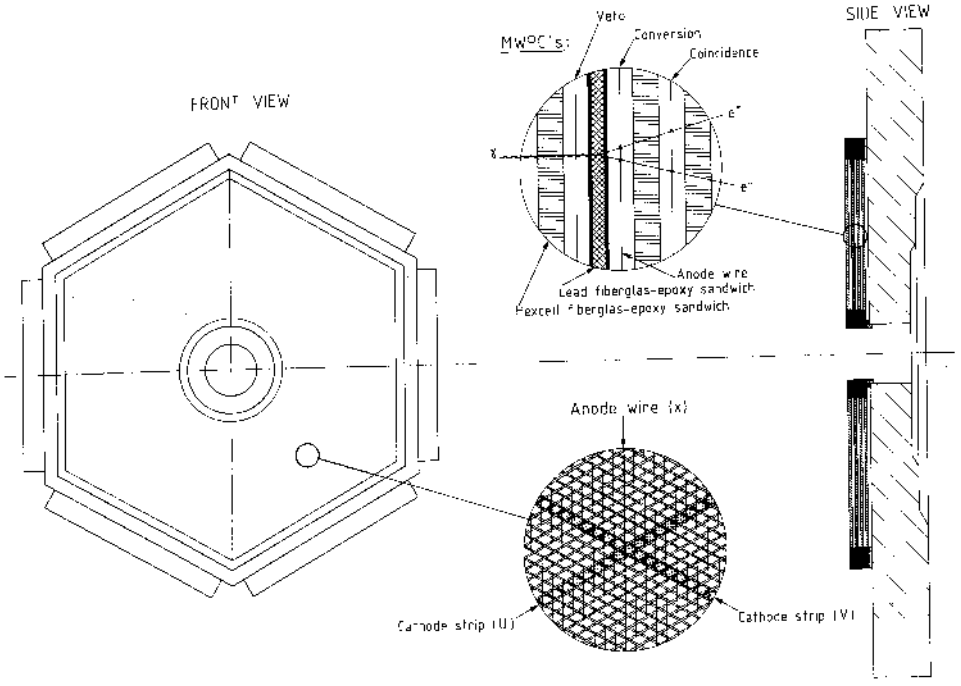

Fig. 5. Position sensitive γ detector to be installed in the endcaps

Table 5. Characteristics of one endcap detector chamber

Anode cathode gap	5 mm
Anode wire spacing	4 mm
Cathode strip spacing	4 mm
Cathode anode angle	± 60°
Number of anode wires	320
Number of cathode strips	2 x 320
Sensitive area	1.3 m^2

Table 6. Performance of γ position detectors

	Spatial resolution	Angular resol.(a)	Solid angle(b)	Conv. Prob.(c)	Det. Efficiency
Endcap	± 2 mm	± 5 mrad	20	40%	8%
Cylind.	± 5 mm	± 9 mrad	50	40%	20%

(a) Combined with reconstructed vertex
(b) Percentage of 4π
(c) Assuming γ ray normal incidence

Experimental data obtained at SIN and results of a shower simulation program lead to the expected performance summarized in table 6 for γ energies $\gtrsim$ 100 MeV.

Pair spectrometer

With the insertion of a γ conversion foil before one of the inner cylindrical chambers, the outer part of the detector can be turned into a pair spectrometer. Different solutions have been considered depending on how the emphasis has to be shared between good spatial resolution and good energy resolution of the γ and the charged prongs resolutions. As example we describe a scheme providing γ detection with good spatial resolution but medium energy resolution. A 0.2 radiation length converter would be inserted before Q_2 and Q_2, P_1, Q_3 and P_2 used for tracking the generated e^+e^- pair. It would lead to an energy resolution of ± 10% for γ energies of about 200 MeV. The γ conversion point could be determined to ± 1 mm. Together with the resolution in the determination of the annihilation vertex from the charged particles, the γ direction would be determined within to ± 5 mrad. The single γ detection probability should be 5% (10% conversion probability *50% of 4π solid angle). In this scheme, however, the resolution on the momentum determination of charged particles would be reduced to ±7% at 500 MeV/c.

Monte-Carlo simulation

Using the characteristics of the charged particle and γ position sensitive detectors given in earlier sections, we have carried out Monte-Carlo simulations of different possible annihilation channels. This was done with a double purpose: firstly, to test the programs that have been written either to reconstruct trajectories from the wire hits or to study the kinematics of the events; secondly, to determine the statistical significance with which predetermined resonances can be established and, at the same time, to estimate the mass resolution attainable. Reconstruction of a Monte-Carlo event is illustrated in fig. 6(b) and compared with the initial configuration in fig. 6(a).

The procedure followed and the results obtained are illustrated with the study of the annihilations

$$\bar{p}p \to \gamma B \quad (B \to \pi^+\pi^-)$$

where B stands alternatively for one of two resonances, decaying isotropically into $\pi^+\pi^-$, with masses of 1395 and 1646 MeV and widths Γ = 0 MeV.

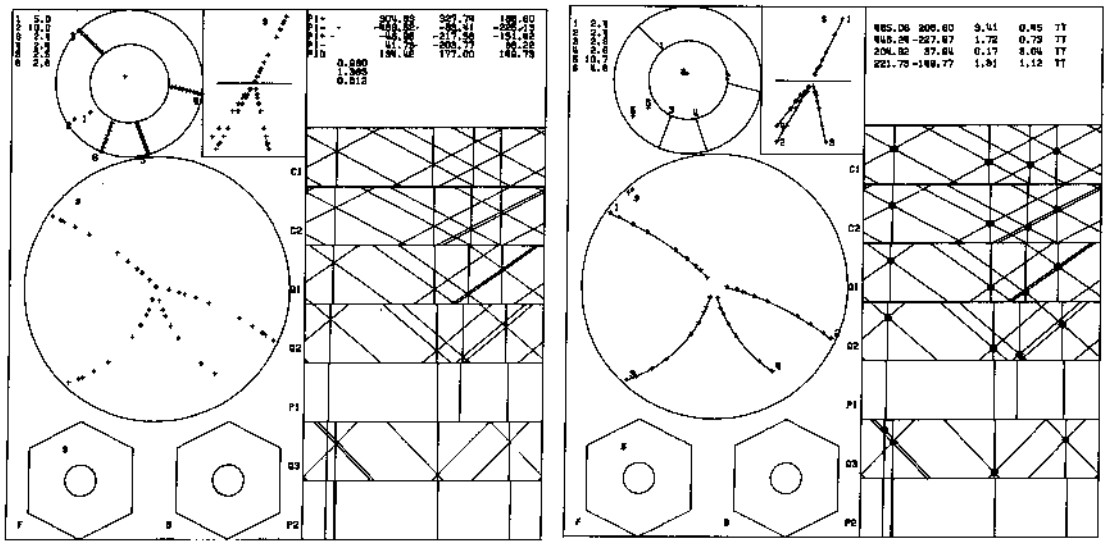

(a) (b)

Fig. 6. Monte-Carlo simulated $\bar{p}p \to 2\pi^+2\pi^-\pi^0$ event in the ASTERIX detector (a) and its reconstruction (b). Small circle: tracks in the XDC. Large circle and insert: tracks in the MWPC's. Bottom: γ induced hits in the endcap detectors. Right: anode and cathode hit wire patterns and reconstructed crossing points.

They should appear as enhancements in the $(\pi^+\pi^-)$ effective mass spectrum from annihilations leading to the production of two charged particles and one gamma ray. We will, nevertheless, consider both the case when the γ has been detected and that when it has not been detected. In either case the wanted events will be accompanied by a large background of annihilations into $\pi^+\pi^-\pi^0$, $\pi^+\pi^-2\pi^0$, ... in which no γ or only one γ from π^0 decay has been detected.

A Monte-Carlo sample of events was generated consisting of 2150 γB(1395) and 2500 γB(1646) events which were assumed to correspond, respectively, to 1.15% and 1.34% contributions to the total $\bar{p}p$ annihilation rate. As background events we took the final states: $\pi^+\pi^-\pi^0$ (6.9%), $\pi^+\pi^-2\pi^0$ (9.3%) and $\pi^+\pi^-3\pi^0$ (23.75%), where the numbers within brackets give the contributions to the total annihilation rate estimated by Ghesquière [27] from bubble chamber results. Phase space distributions were assumed everywhere.

The Monte-Carlo sample consisted therefore of 4650 γB and 74500 background events coming from a total of 1.9×10^5 annihilations. They were then treated with the tracking programme to be used for real events; for 22300 events both the π^+ and π^- momenta and the annihilation vertex were determined while an additional associated γ was also found in 9840 of these events.

The effective $(\pi^+\pi^-)$ mass obtained using directly the measured π^+ and π^- momenta for the 22300 events is shown in fig. 7(a). The B signals appear over a large background and with a mass resolution given by a full width at half maximum (FWHM) of about 120 MeV.

The histogram of fig. 7(b), shows the $(\pi^+\pi^-)$ mass distribution from all 22300 events after making a kinematic fit using only the π^+ and π^- momenta (1 constraint fit) under the assumption that the events belong to the final state $\pi^+\pi^-\gamma$. Only events with a fit probability better than 5% have been accepted. In spite of the large background essentially due to misidentified $\pi^+\pi^-\pi^0$ events, the B signals stand out very clearly. The mass resolution is now 60 MeV. An estimate of the number of B events in each enhancement agrees well with those put in the Monte-Carlo sample and known to have passed the reconstruction test.

Introducing afterwards the position of the detected γ's obtained in the subclass of 9840 events, a kinematic fit was made with 3 constraints (only the absolute value of the γ momentum is missing now to determine completely the assumed $\pi^+\pi^-\gamma$ final state). The mass histogram of fig. 7(c) was obtained. It is to be noted not only that the γ information improves significantly the mass resolution - the FWHM is now 40 MeV - but also that the B signals appear now over a negligible background.

We can use the results of the simulation to estimate realistically the branching ratios $\bar{p}p \to \gamma B(\pi^+\pi^-)$ that could be obtained in an experiment with 10^6 annihilations in the target. We consider that a signal is real i.e. does not represent a statistical fluctuation, if it corresponds to a six standard deviation from the expected background. The results of the B(1646) simulation are used; those for the B(1395) being almost identical as can be seen from the histograms of fig. 7.

Using events with 2 charged particles independently of whether one γ has been detected or not and performing a 1C fit on them, we obtain (fig. 7(b)) 950 B(1646) events standing on a background of 180 ± 20 events. The background is estimated from neighbouring bins. The signal would then correspond to (950/20) a 47 standard deviation effect. Since in the simulation a total of 1.87×10^5 $p\bar{p}$ annihilations and a B(1646) branching ratio of 1.34×10^{-2} have been used, an extrapolation of these results to 10^6 annihilations would lead to the observation of a 6 s.d. effect if the branching ratio is 7×10^{-5}. The signal would, however, consist of $\sim$ 2500 events over a background of $\sim 10^5$ events.

The same study based now on the 3C results from events $\pi^+\pi^-\gamma$ with the γ detected lead to a 6σ deviation for a branching ratio of 4.5×10^{-5}. The signal consists now of about 550 events over a background of about 2500 events.

Clearly, although detection of the γ-ray reduces enormously the background, the ratio of signal to background is too small to allow a study of the J^{PC} of the enhancement. To do this a signal to background ratio of ~ 5 is probably necessary, which implies a branching ratio $\sim 1 \times 10^{-3}$.

The results of the Monte-Carlo simulation just described and similar ones carried out for annihilations $\bar{p}p \to \pi^0 B(\pi^+\pi^-)$ and $\bar{p}p \to \gamma B(\pi^+\pi^-\pi^0)$ agree to a good approximation with those given in the proposal on the basis of simpler considerations. They are reproduced in table 7.

From the Monte-Carlo simulation we arrive at the following conclusions:

(a) Effects (resonances?) occurring with a frequency 10^{-4}-10^{-5} per annihilation can be detected with $\gtrsim$ 6 standard deviations above background. Nevertheless, a proper spin-parity determination would require the frequency not to be much below $10^{-3}/\bar{p}$.

(b) Mass resolutions given by a full width at half maximum $\sim$ 40 MeV or better should be possible.

(c) Kinematic fitting of events appears to be essential, particularly when looking for weak signals; it not only decreases enormously the background but also improves significantly the uncertainties in the measured quantities.

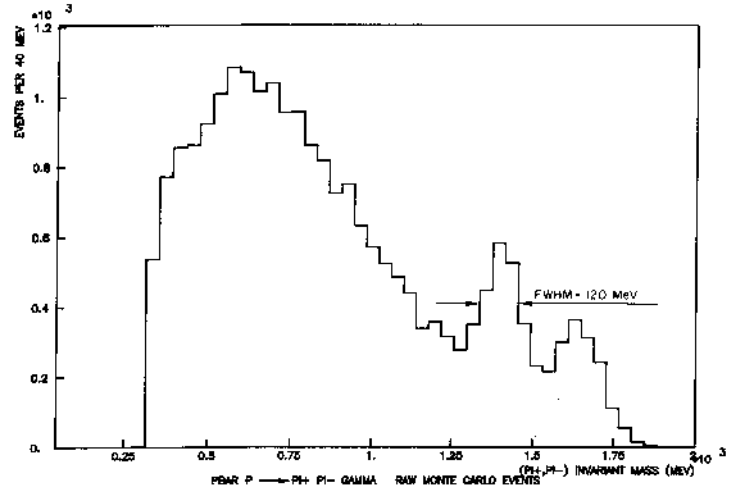

(a) All reconstructed $\pi^+\pi^-$ pairs selected

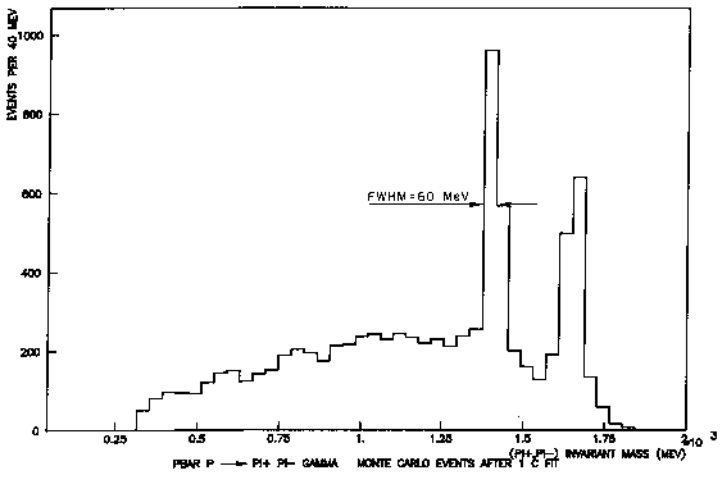

(b) Only $\pi^+\pi^-$ pairs selected that fit the $\bar{p}p \to \gamma\pi^+\pi^-$ hypothesis (1C fit)

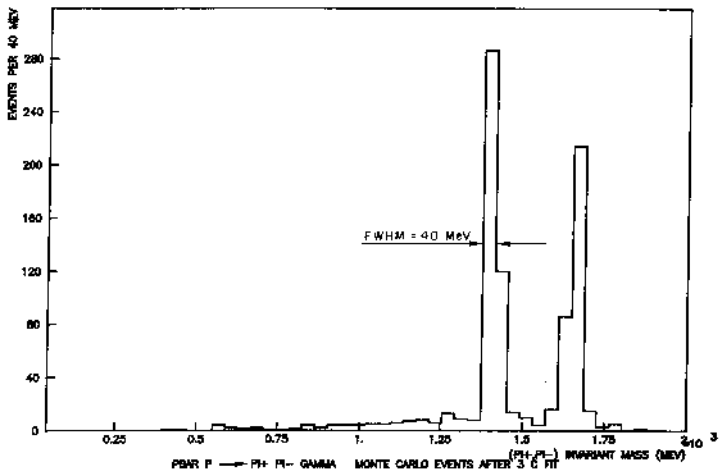

(c) $\pi^+\pi^-$ pairs after kinematical fitting employing also the detected γ-direction (3C fit)

Fig. 7. Distributions of the invariant mass of $\pi^+\pi^-$ pairs in Monte-Carlo generated annihilations $\bar{p}p \to \gamma B_{1,2}$ with $B_{1,2} \to \pi^+\pi^-$ (mass of $B_{1,2}$ = 1395 and 1646 MeV, respectively) for different event selection criteria. The signal events are superimposed on a background assumed to originate from $\bar{p}p \to n\pi^0\pi^+\pi^-$ events.

Table 7. Examples of number of events and branching ratios that could be obtained in an experiment with 10^8 stopped antiprotons

Final state	B.R. $\times 10^2$	Mass of B (GeV)	B.R. a)	Efficiency for charged particles $\times 10^2$	No. events $\times 10^{-3}$	π^0 (γ) effic. $\times 10^2$	No. of events $\times 10^{-3}$
$\pi^+\pi^-$	0.37			50	180	-	-
$\pi^+\pi^-\pi^0$	7			25	1750	10	175
π^+B^- $\rightarrow \pi^-\pi^0$		1.0	2×10^{-5}	25	0.5	10	0.05
π^0B^0 $\rightarrow \pi^+\pi^-$		1.0	2×10^{-5}	25	0.5	10	0.05
γB^0 $\rightarrow \pi^+\pi^-$		1.48	6×10^{-5}	25	1.5	30	0.45
$\pi^+\pi^-$ MM	36			25	6400	-	-
$\pi^+\pi^-B^0$ $\rightarrow \pi^0\gamma$		0.8	1×10^{-3}	25	-	2	0.60
$2\pi^+2\pi^-$	7			6	420	-	-
π^+B^- $\rightarrow 2\pi^+\pi^-$		1.4	2.3×10^{-4}	6	1.6	-	-
γB^0 $\rightarrow 2\pi^+2\pi^-$		1.35	10^{-4}	6	0.6	30	0.18
$2\pi^+2\pi^-\pi^0$	17			6	1000	10	100
π^+B^- $\rightarrow 2\pi^-\pi^+\pi^0$		1.55	5×10^{-4}	6	3.6	10	0.36
π^0B^0 $\rightarrow 2\pi^+2\pi^-$		1.5	2×10^{-4}	6	1.44	10	0.15
$2\pi^+2\pi^-$ MM	21			6	1260	-	-
$2\pi^+2\pi^-B^0$ $\rightarrow \pi^0\gamma$		0.8	3×10^{-3}	6	-	2	0.33

a) These branching ratios correspond to the indicated masses for the B-system. These masses correspond, in general, to the most unfavourable situation. Smaller values of B.R. would be obtained for other masses within the available phase-space limits.

Before ending we should remark that little mention has been made in the presentation of channels containing a $K\bar{K}$ pair, although their importance in spectroscopy studies has been stressed. These channels are, however, extremely rare to be detected easily with sufficient statistics. A microprocessor presently under construction at Orsay is expected to allow to trigger on K_S^0's as well as on other topologies of particular interest.

REFERENCES

[1] I.S. Shapiro, Phys. Rev. 35C (1978) 129;
W. Buck, C. Dover and J.M. Richard, Ann. Physics 121 (1989) 47.

[2] C. Dover and J.M. Richard, Proceedings IV European Antiproton Symposium (1978) CNRS, edited by A. Fridman, Vol. 1, 43.

[3] K. Fransson, Proceedings of this Workshop.

[4] T. Barnes, Proceedings of this Workshop.

[5] See C.E. Carlson, J.J. Coyne, P.M. Fishbane, F. Gross and S. Meshkov, Phys. Lett. 99B (1981) and refs therein.

[6] (a) J.F. Donoghue, K. Johnson and B.A. Li Phys. Lett. 99B (1981) 416;

(b) T. Barnes, Z. Phys. C10 (1981) 275.

[7] D. Robson, Nucl. Phys. B130 (1977) 328.

[8] J.F. Donoghue, Invited Talk at the "Orbis Scientiae" Conference, F. Lauderdale, FLA, Jan. 1981, to be published.

[9] J.D. Bjorken, Proc. Int. Conf. on H.E. Physics, Vol. 1, p. 245, Geneva 1979.

[10] H.J. Lipkin, Phys. Lett. 109B (1982) 326.

[11] J.F. Donoghue, Proceedings A.P.S. Particles and Fields Division meeting Santa Cruz, Cal., September 1981.

[12] B. Berg and A. Billoire, Phys. Lett. 114B (1982) 324.

[13] V. Novikov, M. Shifman, A. Vainshtein and V. Zakharov, Nucl. Phys. B191 (1981) 301.

[14] P. Pascual and R. Tarrach, Phys. Lett. 113B (1982) 495.

[15] T. Barnes and F.E. Close, Rutherford Appleton Laboratory preprint RL 82-037-1982.

[16] R.J. Jaffe, Phys. Rev. D15 (1977) 267.

[17] K. Johnson and C.B. Thorn, Phys. Rev. D13 (1976) 1934; R.L. Jaffe, Phys. Rev. D17 (1978) 1444.

[18] P. Frenkiel et al., Nucl. Phys. B47 (1972) 61 and refs therein.

[19] C. Daum et al., Phys. Lett. 89B (1980) 286.

[20] Ph. Gavillet et al., Phys. Lett. 69B (1979) 119.

[21] C. Dionisi et al., Nucl. Phys. B169 (1981) 1.

[22] J.S. Rosner, Phys. Rev. D24 (1981) 1347.

[23] J.A. Dankowych et al., Phys. Rev. Lett. 46 (1981) 580.

[24] R. Armenteros et al., CERN/PSCC 80-101.

[25] U. Gastaldi, Proceedings of this Workshop.

[26] J.L. Bertrand et al., Invited paper, Int. Conf. on Experimentation at LEP, University of Uppsala, 16-20 June 1980 and refs therein.

[27] C. Ghesquière, Proceedings , Symposium on $N\bar{N}$ interactions, Liblice - Prague, June 1974, Ed. L. Montanet, p. 436.